

A Statistically Driven Spectral Method for Deriving Reservoir Properties Using 3D Seismic Data and Well Log Suites

V. B. Olaseni^{1*}, Y. S. Onifade¹, J. O. Airen² and L. Adeoti³

¹*Department of Physics, Federal University of Petroleum Resources Effurun, Nigeria.*

²*Department of Physics, University of Benin, Benin City, Nigeria.*

³*Department of Geoscience, University of Lagos, Lagos, Nigeria.*

Authors' contributions

This work was carried out in collaboration between all authors. Author VBO designed the study, performed the statistical analysis, wrote the protocol and wrote the first draft of the manuscript. Authors YSO and JOA managed the analyses of the study. Author LA managed the literature searches. All authors read and approved the final manuscript.

Article Information

DOI: 10.9734/AJR2P/2018/v1i124588

Editor(s):

(1) Sebahattin Tuzemen, Professor, Department of Physics, Faculty of Science, Ataturk University, Turkey.

Reviewers:

(1) Muhamamd Tayyab Naseer, Quaid-I-Azam University, Pakistan.

(2) Hector Enrique, Sinaloa University, Mexico.

Complete Peer review History: <http://www.sciencedomain.org/review-history/23928>

Original Research Article

Received 16th January 2018

Accepted 27th March 2018

Published 2nd April 2018

ABSTRACT

A statistically driven spectral method was carried out on 3D seismic data and well logs in "VIC" Field within the Niger Delta with the aim of deriving reservoir properties and delineating stratigraphic features using edge detection attributes like coherence so as to have a better and clearer view of subsurface structure of a reservoir interval that possesses hydrocarbon using Spectral method.

A suite of data consisting of seismic sections and composite logs comprising Gamma-ray, Resistivity, Spontaneous Potential, Sonic Time and Porosity logs (density and Neutron) were utilized to identify reservoir interval on log signature across wells 4 and 5 and the reservoir interval obtained was between 11,164 feet and 11,196 feet. Edge detection attribute like coherence was computed from the amplitude data in time domain and transformed to frequency domain using Fourier Transform tool in MATLAB. In order to display well log in time, well to seismic tie was carried out using check shot data which was used as time to depth relationship.

*Corresponding author: E-mail: olaseni.victor@fupre.edu.com;

The analysis of the spectral domain shows distinct bright spots that vary with measured depth due to variation in fluid and formation properties. The results led to an enhancement of seismic data interpretation in the field of study due to a spectral technique method that was applied to calculate the frequency slices. The results indicate that the spectral domain in coherence attributes revealed better geological features and the reservoir character such as faults and fractures. Frequency domain gives better geological maps as it is used to filter data, which means it is an enhancement of hidden features in time domain and gives a smoother variation of the features that has low frequency values. A reservoir with low frequency values is a sandy environment showing stratigraphy features. Hence, the reservoir is suspected to be a channel fill reservoir. This implies that Spectral domain (frequency) defines major geological areas of the "VIC" field and gives much clearer image of the reservoir features within the field than in time domain.

Keywords: Spectral method; coherence; VIC field; discrete fourier transform.

1. INTRODUCTION

The application of the seismic spectral method to the identification of stratigraphic features is an approach to understanding the geometry of stratigraphic features, using the edge detection attributes like coherence in time and frequency (spectral) domain [1]. Edge detection refers to the process of identifying and locating sharp discontinuities in an image [2]. The discontinuities are abrupt changes in pixel intensity which characterizes boundaries of objects in a scene. There are extremely large numbers of edge detection operators available, each designed to be sensitive to certain types of edges. Edge detection techniques include derivative methods, Hilbert transform, coherence, semblance and other correlation techniques [4]. The coherence attribute measures trace-to-trace similarity (including changes in trace amplitudes) and reveals faults in time slices parallel or perpendicular to stratigraphic bedding and it reveals thick channels that create lateral changes in waveform [5].

Spectral decomposition is a tool which is widely used in the oil industry for identification of discontinuities like faults, fractures, etc which are difficult to identify in time domain seismic data [6]. Spectral decomposition of seismic data is a mathematical tool that uses the discrete Fourier transform (DFT) to image thickness variability [7]. It provides a novel means of utilizing seismic data and DFT for imaging and mapping temporal bed thickness and geologic discontinuities over large 3D seismic surveys. Phase spectra indicate lateral geologic discontinuities while amplitude spectra delineate temporal bed thickness variability [8].

In all of these, relatively thin stratigraphic intervals of sand are seldomly considered. Often

on seismic sections, structural styles like anticlines and faults are displayed together with thick stratigraphic bundles of sands [9]. This work takes a closer look at the thin sands by analyzing the seismic attributes within the facies to establish some quantitative interpretations for them. In addition to conventional trends, a 'spectral visualization' is introduced to see the responses of these attributes in the frequency domain. A comparison of the time domain response to the spectral domain in time-frequency would be investigated. In achieving all of these, a combined approach of petrophysics and seismic interpretation would be used so as to delineate hydrocarbon prospect of the field. In this study, a statistically driven method using frequency method (Discrete Fourier Transform Tool) was applied to the seismic attributes so as to identify reservoir interval and to delineate stratigraphic features within the 'VIC'-field.

The aim of this study is to delineate stratigraphic features using edge detection attributes so as to have a better and clearer view of subsurface structure that possesses hydrocarbon reservoir with the use of frequency method (Discrete Fourier Transform).

The main objective of the study is to develop a robust technique for mapping subtle stratigraphic units which are usually masked after normal data interpretation using the edge detection techniques of coherence algorithms which act on the seismic data and is devoid of horizon picker biases.

1.1 Statement of Problem

The analysis of the subsurface features using Time Domain method in the past study was unable to provide a much better and clearer image of the subsurface rock layers due to its

poor quality. This now informed the application of frequency method in order to obtain a better resolution of the subsurface rock layers and delineate the prospective zones for hydrocarbon reservoir.

1.2 Field Description and Geology of the Study Area

The study area of this research is situated in the "VIC" field in Niger Delta, Nigeria as shown in the Fig. 1, which is one of the world's major hydrocarbon provinces.

The Niger Delta is the most important sedimentary basin in Nigeria considering its size, thickness and the economic importance. The Delta covers an area of about 105,000 km² [1]. The Niger Delta is situated on the Gulf of Guinea on the West Coast of Africa. It is located at the southeastern end of Nigeria, bordering the Atlantic Ocean and extends from latitudes 4° to 6°N and longitudes of 3° to 9°E. The basin is bounded to east by the Calabar Flank, to the West, it is bounded by the Benin Basin, to the

South by the Gulf of Guinea and to the North by Older (Cretaceous) tectonic structures such as the Anambra Basin, Abakiliki Anticlinorium and Afikpo Syncline [8].

1.3 Seismic Data

The data used for this project were obtained from Chevron Nigeria Limited with permission of the Department of Petroleum Resources (DPR), Lagos. There are six well logs on the VIC-field but the well log data used are from Well logs 4 and 5 of the field. The log data consist of Gamma, Resistivity, Sonic Time, Neutron and Density logs. The seismic data comprise 3D migrated pre-stacked Seismic data (SEG Y), check shot data and survey map.

1.4 Equipment

Equipment used are Three-component (3C) Hydrophones, Vibroseis energy sources, Seismographs and well-log equipments such as Snow Wolf-5, EILog-06 and Casing Collar Locator.

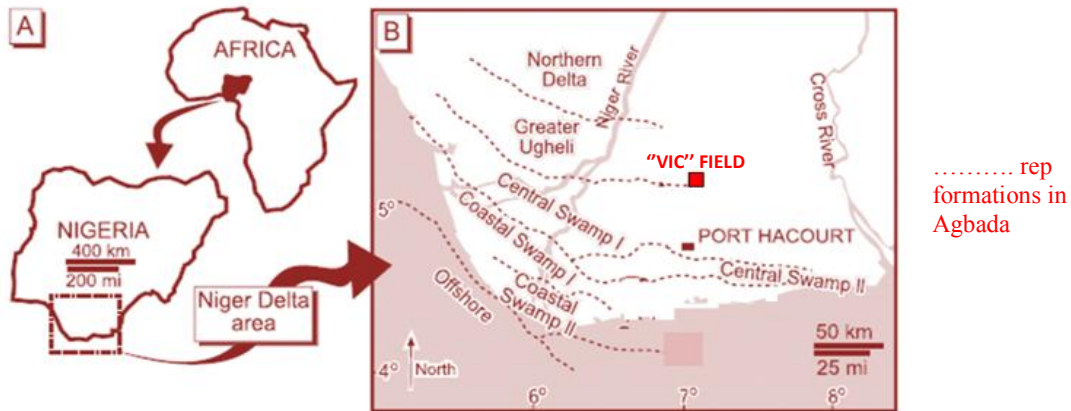


Fig. 1. Map of Niger-delta showing location of the study area [9]

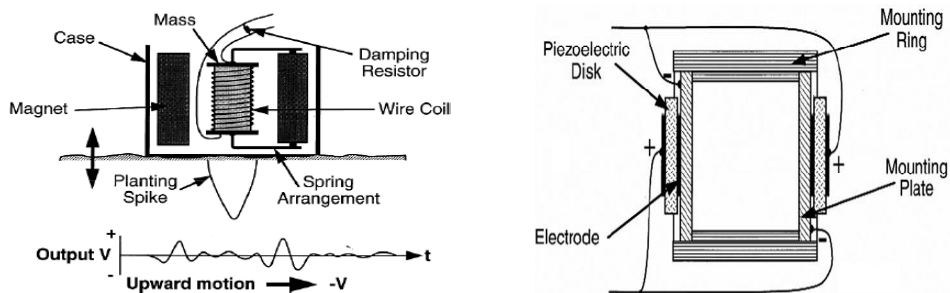


Fig. 1.1. Schematic Representation of: (i) Geophone and (ii) Hydrophone (Modified from [3])

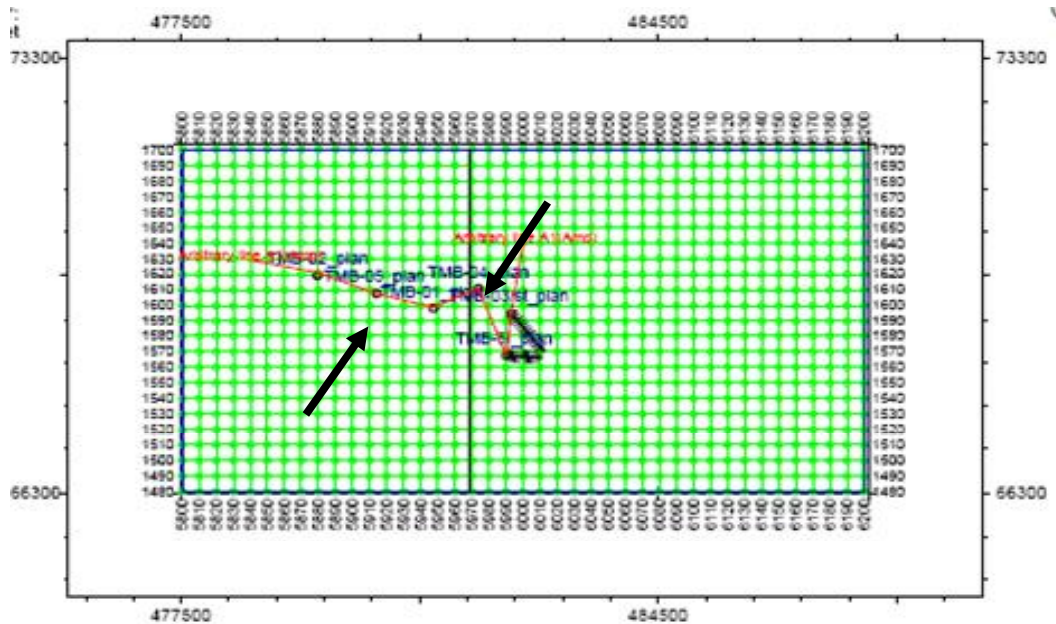


Fig. 2. Base Map of 3-D Seismic Showing all Wells (well 4 and 5 are shown as TMB 04 and 05 with Arrows An Arbitrary Red Line Drawn to Connect the Six Wells in Field (courtesy: Chevron Nig Ltd)

1.5 Base Map

Fig. 2 is the survey map of the field data given by Chevron Corporation which is the Base map of 3-D seismic showing all wells. The map covers all the six wells with well 3 and well 6 at greater depths deviated, the two arrows shown in the Fig. 2 are the wells 4 and 5 which are indicated as TMB 04 at coordinate (5975, 1612) and TMB 05 at coordinate (5915, 1610). The seismic data comprise 400 inlines and 200 crosslines.

2. FIELD METHODOLOGY

2.1 Data Acquisition

The field methodology used for the acquisition of data was Seismic reflection method in which it was carried out on onshore (on land)

environments. However, the information about the subsurface geology, physical rock properties and layers attitude of the environment was inferred from the reflected wave travel-time between the source and its arrival at the receivers as seen in Fig. 2.1.

2.2 Data Processing

The data acquired was processed using the combination of conventional semblance algorithms and non-conventional technique of the discrete Fourier transform and this was done within Matlab software. This is to delineate stratigraphic features using edge detection attributes so as to have a better and clearer view of subsurface structure that possesses hydrocarbon reservoir using DFT.

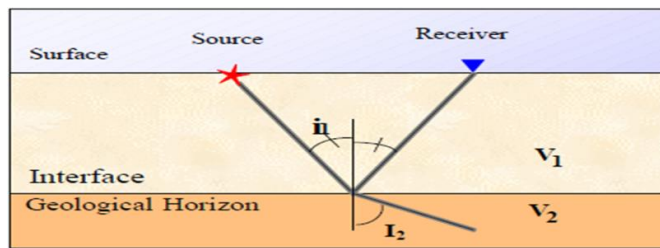


Fig. 2.1. Fig 2.5 Reflected and Refracted P and S-Wave [10]

3. THEORY

3.1 Discrete Fourier Transform (DFT)

The Discrete Fourier Transform (DFT) is the digital equivalent of the continuous Fourier transform and is expressed as

$$f(w) = 2 \sum_i f(t)e^{-iwt} \quad (1)$$

Where w is the Fourier dual of the variable 't'. If 't' signifies time, then 'w' is the angular frequency. Which is related to the linear (temporal) frequency 'f'. Also, $F(w)$ comprises both real $F_r(w)$ and imaginary $F_i(w)$ components [11].

4. DISCUSSION OF RESULTS

4.1 Lithology Identification

In order to delineate the various lithologies, the Figs. 3 and 4 show the entire data sets of four logs plotted against depth. Reservoir intervals are indicated on both Figs (in a box) with a characteristic of low Gamma values and high resistivity values (which is likely to be HC

saturation zone). Thus, the reservoir interval is at the measured depth of 11,164 ft to 11,196 ft for well 4 while that of well 5 is from 11,048 ft to 11,097 ft.

4.2 Selection of a Thin Sand Interval

Figs. 5 and 8 are the plots of four logs (Gamma, Resistivity, Porosity, Sonic Time and Densitylogs), that are at the measured depth interval of 11,164 ft to 11,196 ft for well 4 while that for well 5 is 11,048ft to 11,097ft. These logs were plotted within the reservoir interval of consideration and they were selected as a case study for the entire sand sequence that is yielding in each well showing the formation response. The arrows shown on each plot indicate a distinct sand interval with a characteristic of low Gamma ray values and high Resistivity values within the reservoir interval and the porosity values for this region fall between 22% and 23%. This means that the porosity is very good (according to [2] in *Qualitative Evaluation of Porosity in Reservoir Rocks*, any percentage porosity that is between 20-25 means is very good).

Well 4 (entire data set)

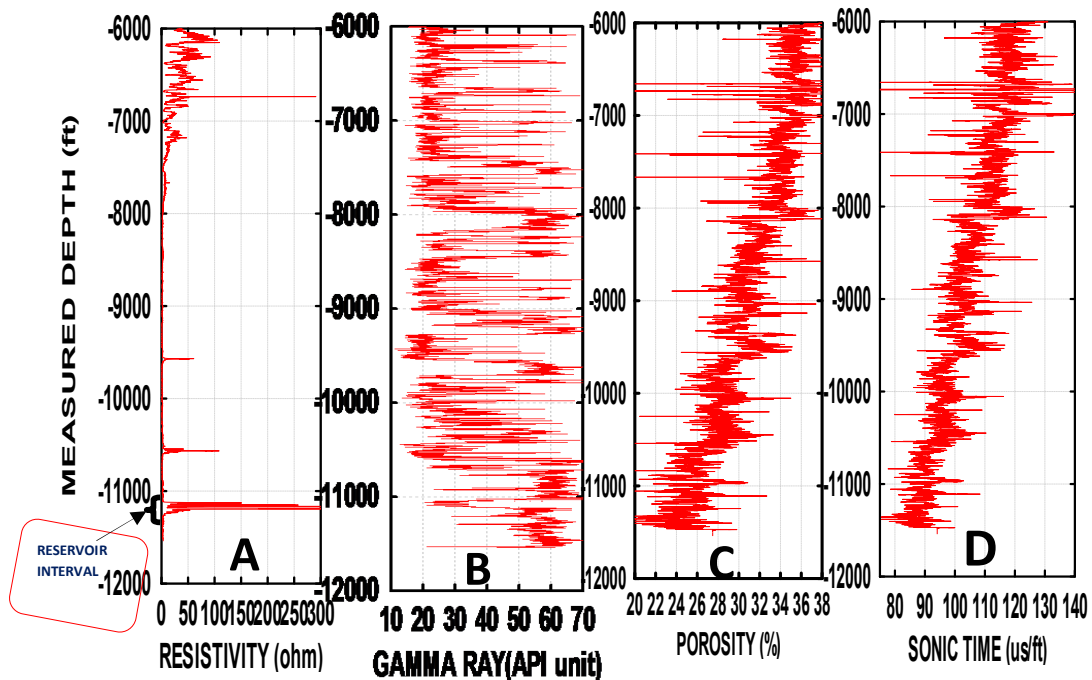


Fig. 3. Logs of (A) Resistivity, (B) Gamma ray (C) Porosity and (D) Sonic Time, respectively for Well 4. The Small Box indicates the Reservoir Interval of the Measured Depth Interval of 11,164 ft to 11,196 ft, Which is Herein Closely Examined Quantitatively

Well 5 (entire data set)

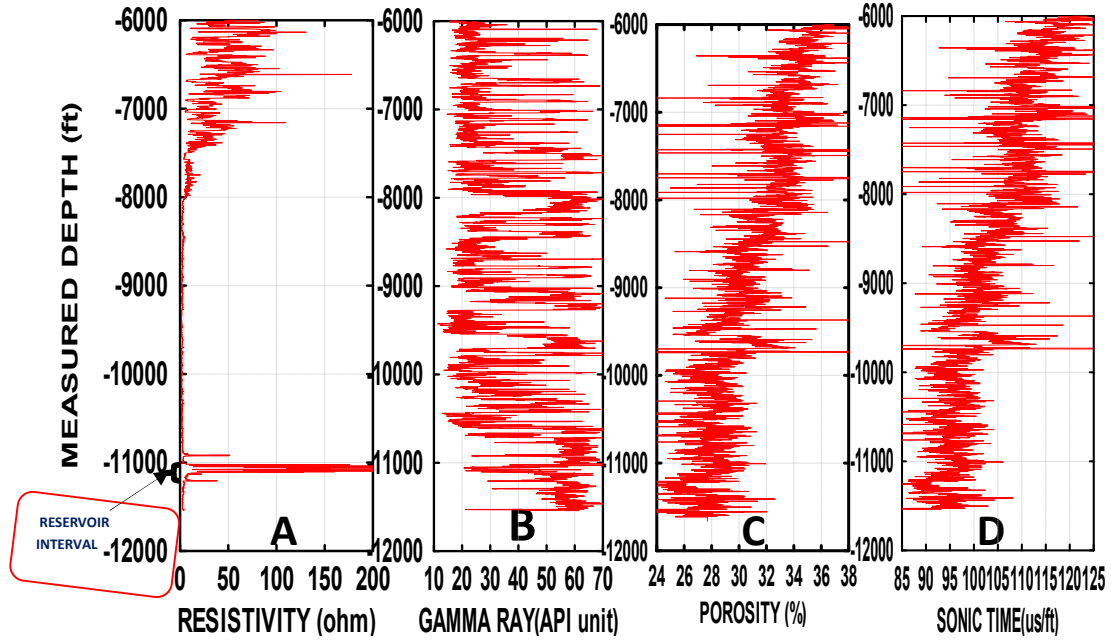


Fig. 4. Logs of (A) Resistivity, (B) Gamma ray, (C) Porosity and (D) Sonic Time respectively for Well 5. The Small Box Indicates the Reservoir Interval of the Measured Depth Interval of 11,048 ft to 11,097 ft which is Herein Closely Examined Quantitatively

Well 4(reservoir interval)

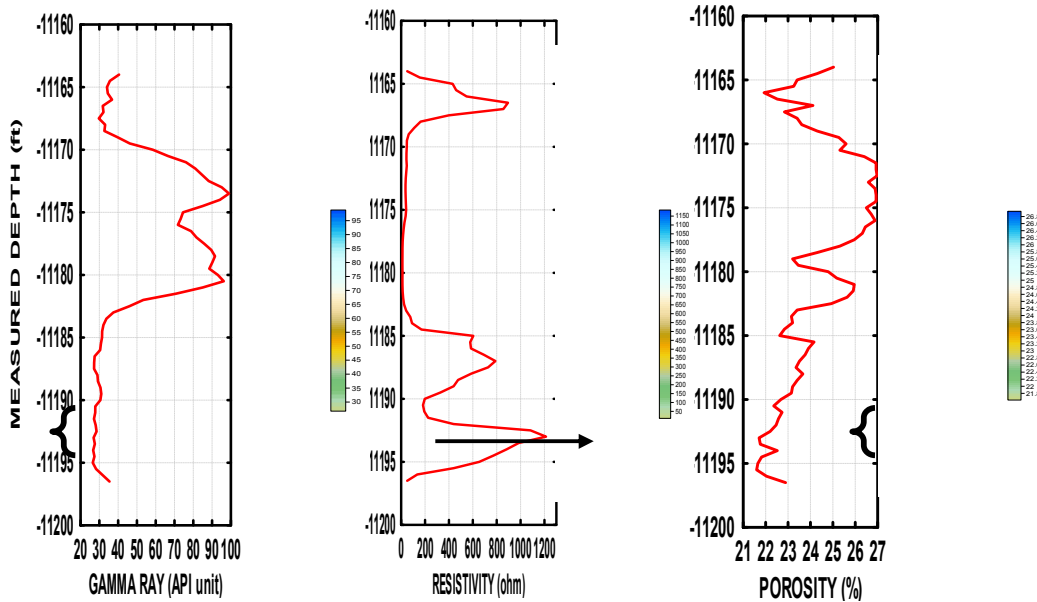


Fig. 5. Logs of gamma ray (GR), resistivity (LLD) and porosity within the depth interval of the reservoir for well 4. Right to each plot is a respective surface map generated to show comparison within the interval, also the legend shows the distribution of the quantities with depth

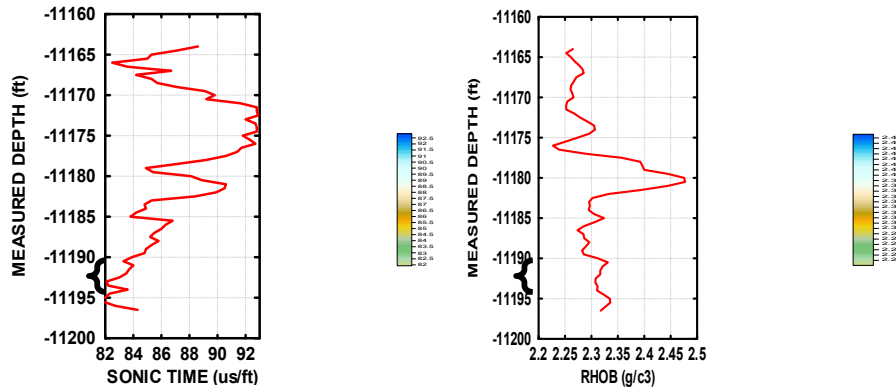


Fig. 6. Logs of sonic time and density (rhob) within the depth interval of reservoir for well 4. right to each plot is a respective surface maps generated to show comparison within the interval, also the legend shows the distribution of the quantities with depth

Well 5 (reservoir interval)

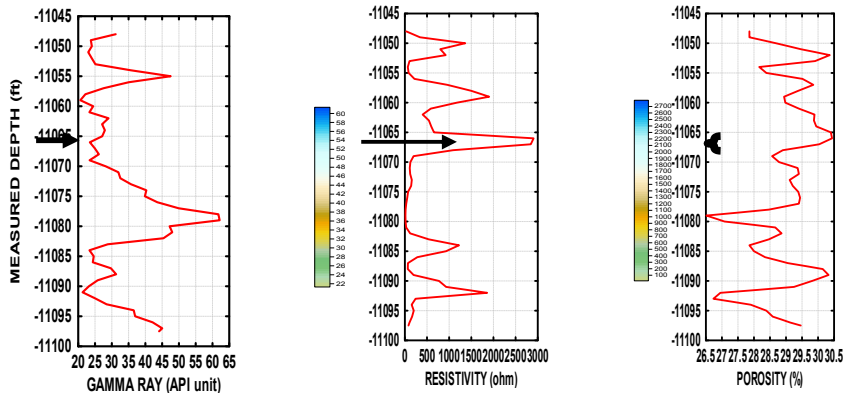


Fig. 7. Logs of gamma ray (GR), resistivity (LLD) and porosity within the depth interval of reservoir for well 5. right to each plot is a respective surface maps generated to show comparison within the interval, also the legend shows the distribution of the quantities with depth

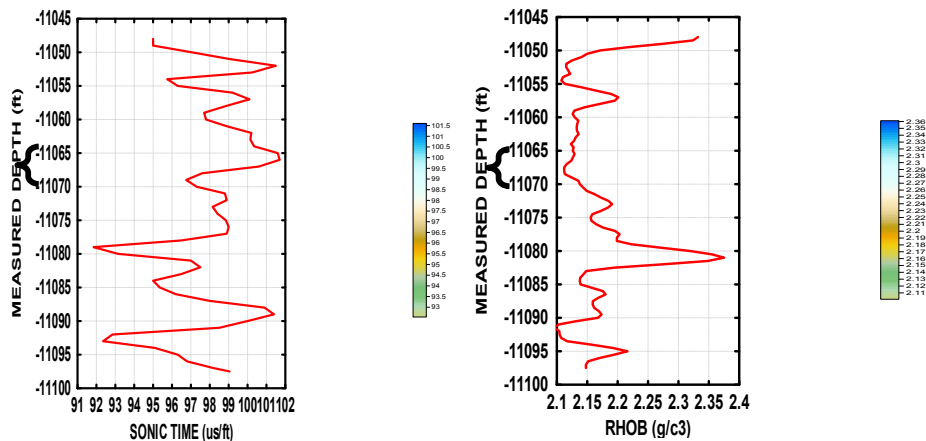


Fig. 8. Logs of sonic time and density (RHOB) within the depth interval of reservoir for well 5. right to each plot is a respective surface maps generated to show comparison within the interval, also the legend shows the distribution of the quantities with depth

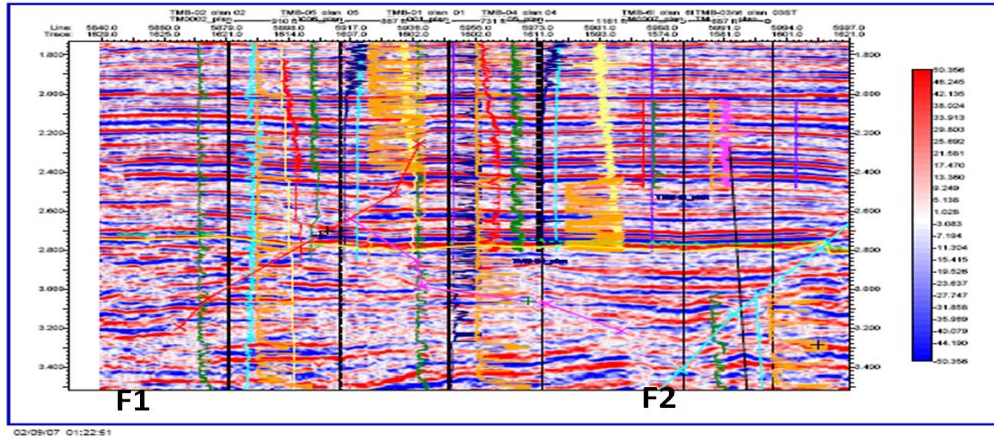


Fig. 9. Seismic Section Showing an Arbitrary Line Indicating Two Major Faults, F1 and F2 Bounding the Wells at the Reservoir Interval under analysis (2.752-2.768 sec). The well Locations are indicated above the seismic section

Right to each wiggle is a respective surface plot generated to show comparison within the reservoir interval while the legend beside it shows the distribution of the quantities with depth.

The reservoir interval of interest at the depth of 11,164 ft (top) and 11,196 ft (bottom) on well log corresponds to 2.752 seconds (top) and 2.768 seconds (bottom) respectively on seismic section using equation

4.3 Seismic Section with the Wells

$$TWT = 2t = \frac{2d}{v} \tag{2}$$

Fig. 9 is a seismic section with an arbitrary line showing two major faults, F1 and F2 bounding the wells at the reservoir interval under analysis (2.752-2.768 sec) and the well locations are indicated above the seismic-section.

This is necessary so as to have a complete picture of the inter-well zones.

4.4 Spectral Analysis of Seismic Attributes Within the Reservoir

5. LINES PLOTS

Figs. 10 to 12 show different geologic features revealed by the different attributes (such as coherence etc), which were computed in time domain and frequency domain. The time domain attributes were converted to frequency domain after being time sliced at every 4 ms within the reservoir interval.

Fig. 10 shows the lines plots of amplitude derived coherence and gamma log plot by DFT using different analysis window centered at top of sand interval. The change in the direction of the phase spectral means that the magnitude plot is perfectly symmetrical about the Nyquist frequency of 50Hz. Therefore, the maximum usable frequency (MUF) in the data is 50Hz and this implies that the useful information in the signal is found in the range 0 to 50Hz as shown on the legend in the frequency maps.

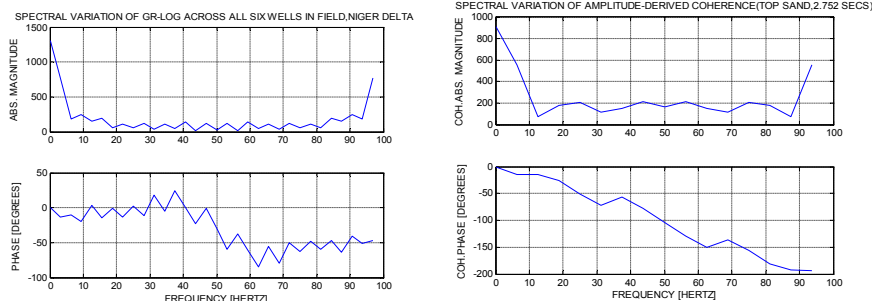


Fig. 10. Lines plots of amplitude derived coherence and gamma log

6. CONTOUR MAPS

Fig. 11 shows the amplitude time map and its contour map at the top of delineated reservoir

(2.752 seconds), also Fig. 12 shows amplitude time map and its contour map at the base of delineated reservoir at 2.768 seconds.

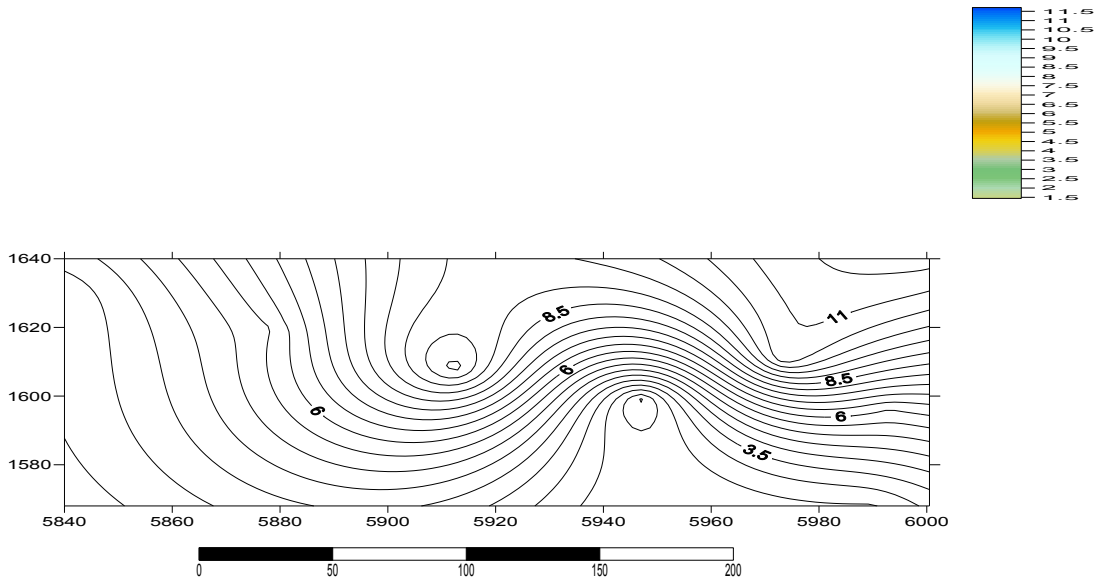


Fig. 11. Amplitude time maps with contour maps at the top of delineated reservoir (2.752 sec)

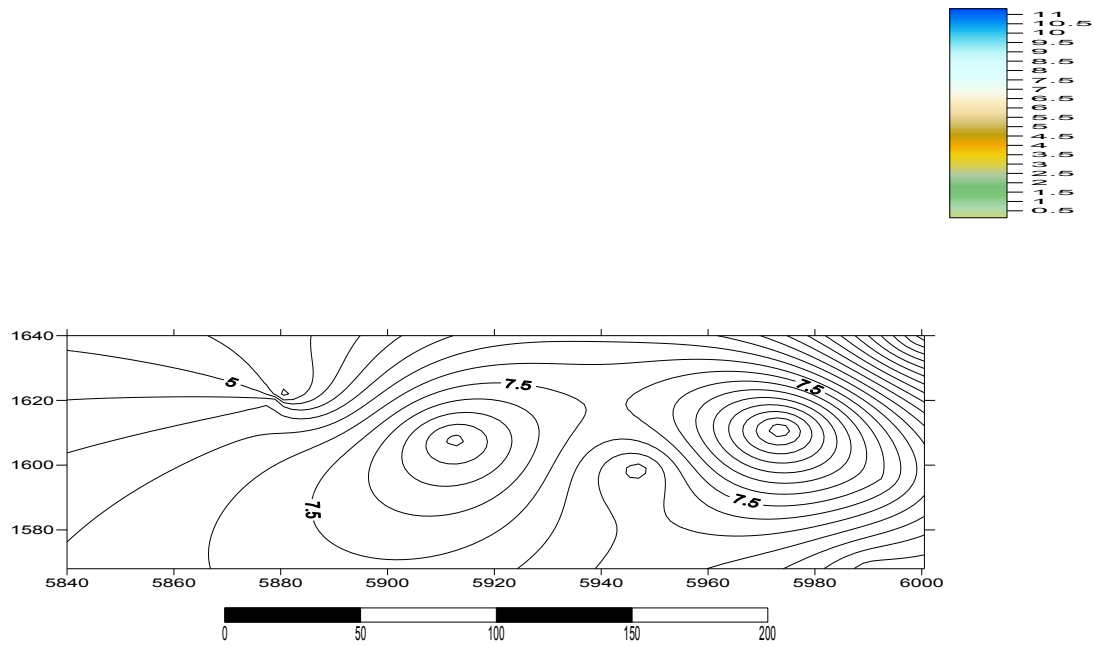


Fig. 12. Amplitude time maps with contour maps at the base of delineated reservoir (2.769)

7. SPECTRAL ANALYSIS MAPS

The computed attributes in Figs. 13 to 17 are so arranged for the purpose of identifying stratigraphic variations that are not evident on field amplitude display bearing the triangle and square symbols. The field amplitude data map (Fig. 13) shows the triangle spot as sandy zone while the Gamma-Ray map and coherence map attribute indicate the presence of sand –shale interface at the same points due to the high frequency values as shown on the legend of the map. There is better edge definition at B (coherence amplitude in time) than at A (original amplitude in time).

The prospective zones in Fig. 17 are not obvious on the amplitude display (Fig. 13), and these prospective zones have the characteristics of low Gamma-Ray values and low frequency values as shown on the legend. Therefore, stratigraphic and structural features can be identified on coherence maps than on the original amplitude data. Fig. 17 also indicates distinct bright spots which are not obvious on the original amplitude display in Fig. 13. Furthermore, these distinct bright spots that displayed on the frequency domain maps vary with depth due to variation in fluid and formation properties.

Stratigraphic features like faults, channel, etc can be observed on the coherence phase map (Fig. 16) than in coherence amplitude in time domain (Fig. 15), and the results displayed in Fig. 16 indicate that the reservoir is a *channel* fill.

Also the map of coherence phase (Fig. 16) indicates lateral continuity and sequence boundaries which reveals bedding discontinuities because the higher the frequencies the sharper the discontinuities.

The frequency map of the coherence (Fig. 17) shows the drilled hydrocarbon zones and potential prospects areas by its low frequency anomaly. Therefore, the results from these coherence maps reveal that processing a coherence attribute in frequency domain rather than relying on horizon picks give better results, then the outcomes of the structural and stratigraphic elements are more evident and well seen, finally this is our area of interest.

Figs. 13 to 17 shows Comparison of Attribute Maps of Original, Gamma and Coherence Amplitude in time domain, Coherence in phase and Coherence in Frequency at Delineated Reservoir.

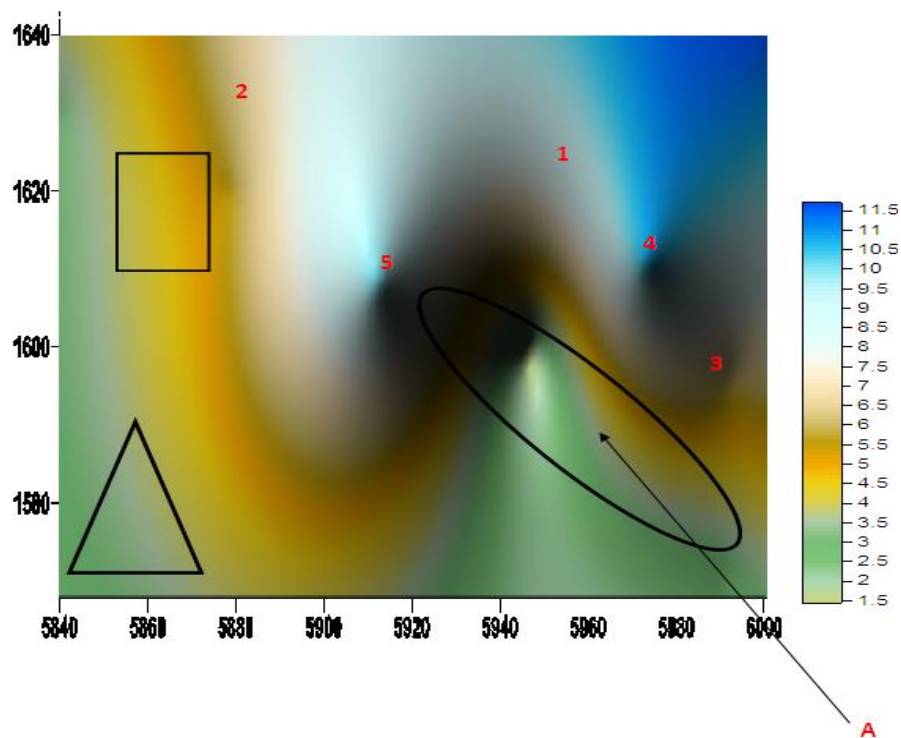


Fig. 13. Original amplitude (Time)

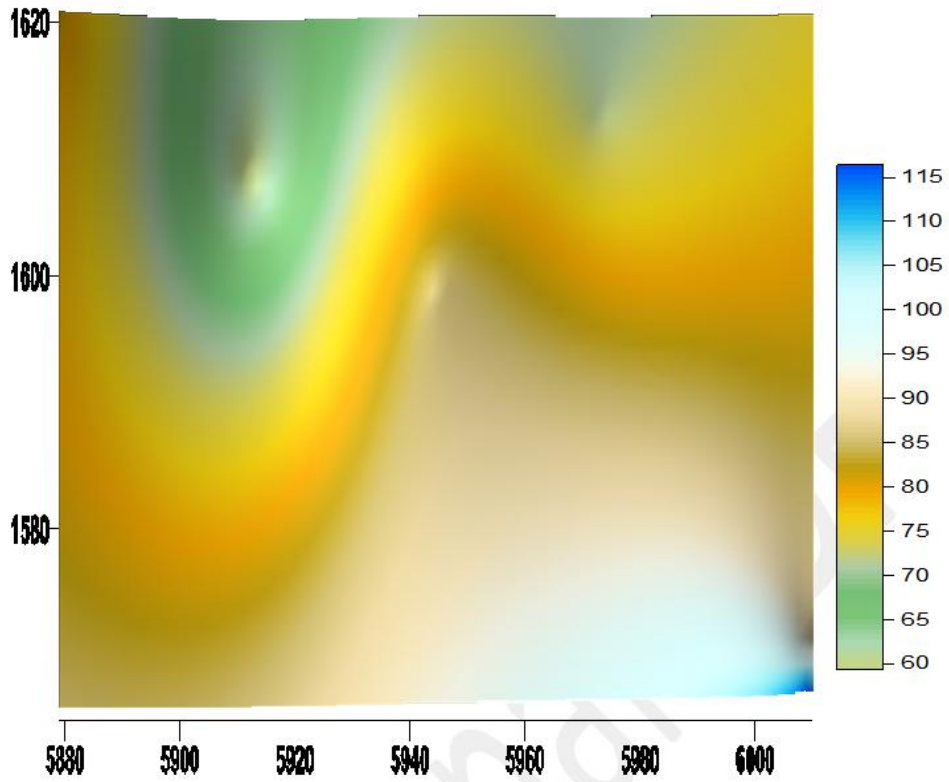


Fig. 14. Gamma amplitude in time domain

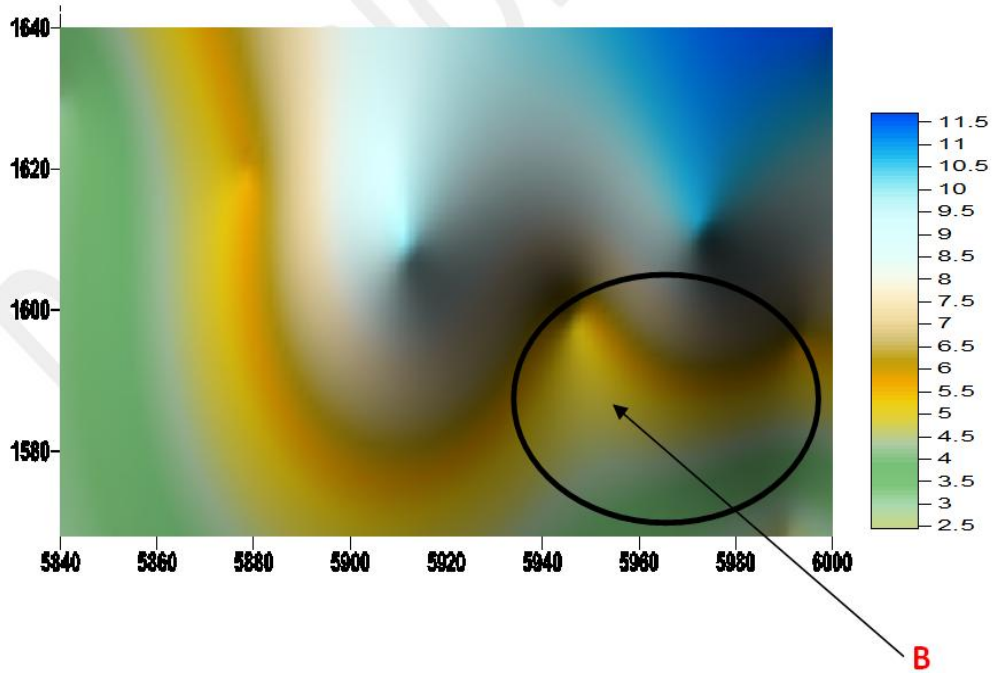


Fig. 15. Coherence amplitude in time domain

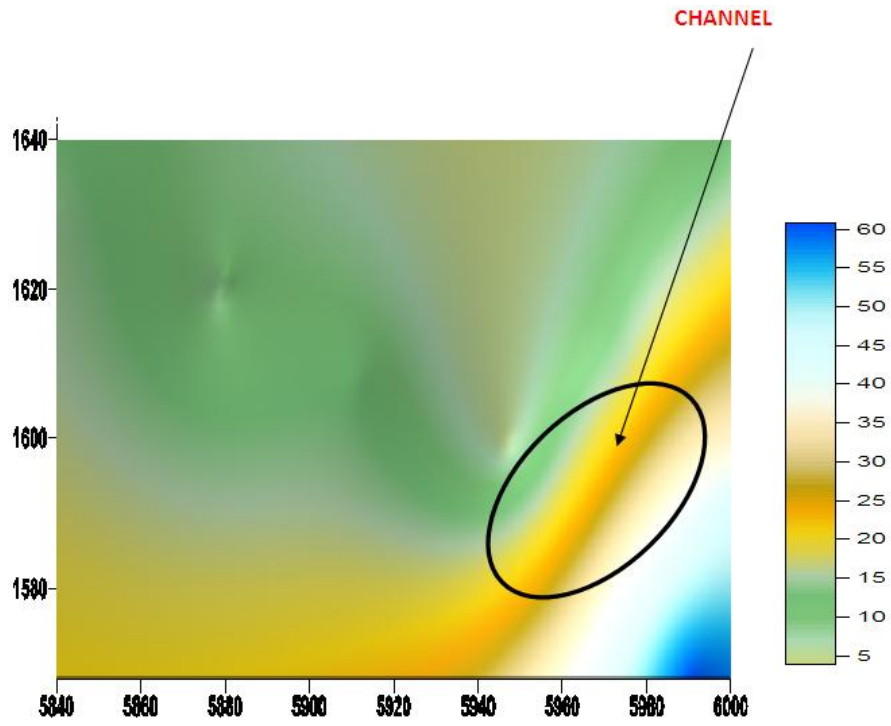


Fig 16. Coherence in phase

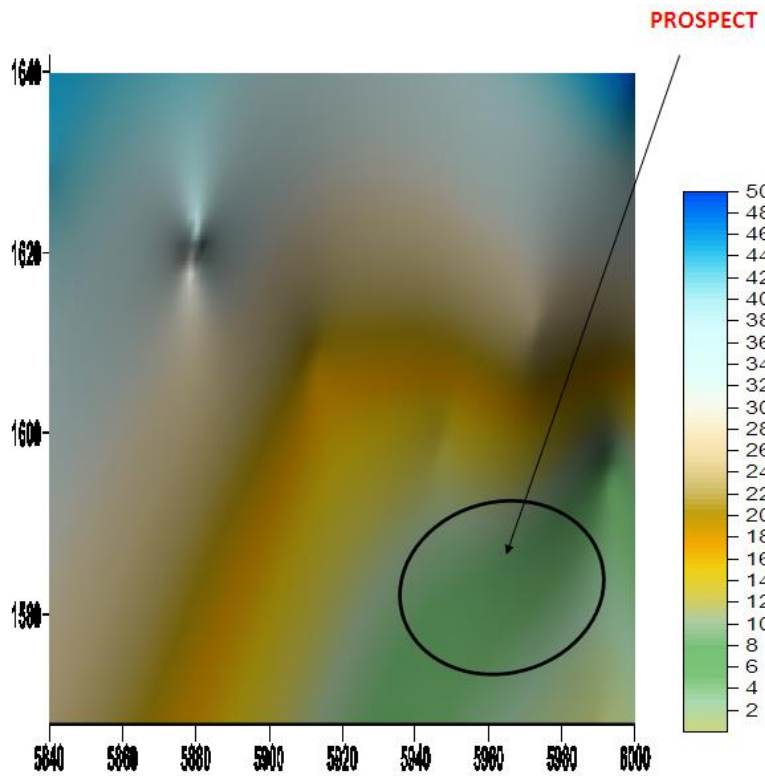


Fig. 17. Coherence in frequency

Table 1. A composite log data within the studied interval [Two way time (TWT) and acoustic impedance (AI) were computed from this data]

md	vd	Gr	LLD	TWT	HOB	AI	Q
-11164.0	11164.0	0.4842	50.6723	-2.7592684	2.2649	20211.8270	25.03047404
-11164.5	11164.5	5.6028	55.9496	-2.7593920	2.2524	20052.5394	24.30769231
-11165.0	11165.0	4.0541	31.1316	-2.7595156	2.261	19600.3475	23.40679953
-11165.5	11165.5	4.4808	60.3127	-2.7596391	2.2679	19123.3880	23.25294118
-11166.0	11166.0	6.7477	47.9607	-2.7597627	2.2764	18740.6172	21.92727273
-11166.5	11166.5	1.8005	94.4689	-2.7598863	2.2831	19010.1684	22.52033493
-11167.0	11167.0	2.1903	56.1526	-2.7600099	2.2854	19287.5536	24.11072664
-11167.5	11167.5	9.7167	98.8385	-2.7601335	2.2714	19592.5444	22.83729216
-11168.0	11168.0	3.0898	62.5815	-2.7602570	2.2669	19789.8424	23.40679953
-11168.5	11168.5	2.6812	08.9391	-2.7603806	2.262	19626.5740	23.61026838
-11169.0	11169.0	9.6523	63.2752	-2.7605042	2.2604	19465.9776	24.30769231
-11169.5	11169.5	46.199	48.0528	-2.7606278	2.2637	19149.2819	25.26599327
-11170.0	11170.0	8.4497	46.8566	-2.7607514	2.266	18714.2857	25.59131403
-11170.5	11170.5	6.5004	44.4623	-2.7608749	2.2545	18771.7228	25.31278027
-11171.0	11171.0	6.1032	43.9966	-2.7609985	2.2521	18915.4569	26.40502183
-11171.5	11171.5	1.0416	47.0437	-2.7611221	2.2523	18612.7660	26.92995690
-11172.0	11172.0	4.6331	42.6582	-2.7612457	2.2673	18490.2460	26.92995690
-11172.5	11172.5	8.2044	38.4447	-2.7613693	2.2784	18373.3670	26.97308934
-11173.0	11173.0	95.1308	36.5091	-2.7614928	2.2924	18257.9564	26.58152174
-11173.5	11173.5	9.0048	36.3115	-2.7616164	2.3049	18204.5929	26.88673139
-11174.0	11174.0	4.1729	37.641	-2.7617400	2.3067	18484.5962	26.92995690
-11174.5	11174.5	84.954	39.5106	-2.7618636	2.2963	18901.6764	26.92995690
-11175.0	11175.0	74.531	41.6487	-2.7619871	2.2739	19337.9791	26.49346405
-11175.5	11175.5	3.3371	37.547	-2.7621107	2.2509	19329.5603	26.71289274
-11176.0	11176.0	1.8236	27.8354	-2.7622343	2.2271	19094.8651	26.88673139
-11176.5	11176.5	8.8215	21.1318	-2.7623579	2.2391	19270.9875	26.44929117
-11177.0	11177.0	1.6681	16.309	-2.7624815	2.2889	19450.3546	26.31619256
-11177.5	11177.5	5.7899	12.8744	-2.7626050	2.3569	19801.4619	25.95695364
-11178.0	11178.0	9.5472	11.4657	-2.7627286	2.3925	20523.8971	25.31278027
-11178.5	11178.5	1.5638	10.8708	-2.7628522	2.3964	20316.5804	24.30769231
-11179.0	11179.0	0.1256	10.5971	-2.7629758	2.3998	20000.0000	23.20141343
-11179.5	11179.5	8.5258	10.6751	-2.7630994	2.4444	19229.4191	23.45784543
-11180.0	11180.0	3.0682	11.055	-2.7632229	2.4755	18516.0758	24.79228150
-11180.5	11180.5	6.2107	10.602	-2.7633465	2.4772	18440.0657	25.17210349
-11181.0	11181.0	5.0387	10.8707	-2.7634701	2.4442	18364.6770	25.95695364
-11181.5	11181.5	0.6806	12.604	-2.7635937	2.3942	18701.0980	25.91160221
-11182.0	11182.0	3.3842	16.8514	-2.7637173	2.3329	19067.0059	25.63737486
-11182.5	11182.5	5.9899	24.2234	-2.7638408	2.3019	19131.9149	24.93552036
-11183.0	11183.0	37.4522	41.9491	-2.7639644	2.2956	19197.2673	23.40679953
-11183.5	11183.5	3.7364	76.4117	-2.7640880	2.297	18978.4559	23.14976415
-11184.0	11184.0	2.1679	90.9456	-2.7642116	2.2948	18722.8715	23.20141343
-11184.5	11184.5	31.485	70.0539	-2.7643351	2.3052	18137.0389	22.83729216
-11185.0	11185.0	1.4149	03.9718	-2.7644587	2.3238	17497.9822	22.62649165
-11185.5	11185.5	0.8152	78.3007	-2.7645823	2.3062	17561.7659	24.16013825
-11186.0	11186.0	30.412	84.7858	-2.7647059	2.286	17626.0163	23.91193511
-11186.5	11186.5	27.4887	92.1741	-2.7648295	2.2736	17858.3343	23.76162791
-11187.0	11187.0	27.2283	89.1167	-2.7649530	2.2849	18096.8280	23.50877193
-11187.5	11187.5	27.192	28.0024	-2.7650766	2.2863	18287.6578	23.35563380
-11188.0	11188.0	28.991	87.0048	-2.7652002	2.296	18482.5234	23.66083916
-11188.5	11188.5	29.2431	76.5039	-2.7653238	2.2898	18427.5393	23.40679953
-11189.0	11189.0	30.5899	39.2133	-2.7654474	2.2823	18372.8814	23.20141343
-11189.5	11189.5	31.0231	328.1038	-2.7655709	2.2855	18577.5493	23.14976415
-11190.0	11190.0	30.5284	197.535	-2.7656945	2.3124	18786.8284	22.67938021

md	vd	Gr	LLD	TWT	HOB	AI	Q
-11190.5	11190.5	27.8348	182.8378	-2.7658181	2.3311	19252.1067	22.36014406
-11191.0	11191.0	27.8062	93.6702	-2.7659417	2.3213	19678.2842	22.73214286
-11191.5	11191.5	27.1328	25.5916	-2.7660652	2.3168	19626.3345	22.57347670
-11192.0	11192.0	28.0307	439.54	-2.7661888	2.3166	19645.7042	22.46706587
-11192.5	11192.5	28.5082	082.764	-2.7663124	2.308	19483.1192	22.19879518
-11193.0	11193.0	26.9369	213.057	-2.7664360	2.3074	19480.0693	21.70767357
-11193.5	11193.5	27.5919	84.6743	-2.7665596	2.3117	19263.0512	21.76277372
-11194.0	11194.0	26.7015	84.1627	-2.7666831	2.3106	19050.8475	22.52033493
-11194.5	11194.5	27.3749	72.8748	-2.7668067	2.3232	19026.6610	21.81773998
-11195.0	11195.0	26.4786	53.7974	-2.7669303	2.3347	18968.7236	21.65243902
-11195.5	11195.5	28.248	39.9078	-2.7670539	2.3358	18920.7420	21.59706960
-11196.0	11196.0	31.8182	34.8619	-2.7671775	2.3264	18873.0025	22.03627570
-11196.5	11196.5	35.3917	50.5399	-2.7673010	2.3177	18896.8421	22.88967972

Table 2. Check shot data provided, courtesy: Chevron; but modified

MD(ft)	TWT(s)	TWT/2(s)
45.00	0.00	0
616.00	200.00	100
1210.50	400.00	200
1837.00	600.00	300
2505.50	800.00	400
3225.50	1000.00	500
3895.50	1200.00	600
4779.00	1400.00	700
5634.52	1600.00	800
6458.00	1800.00	900
7413.94	2000.00	1000
8285.00	2200.00	1100
9197.89	2400.00	1200
10056.74	2600.00	1300
11468.55	2800.00	1400
11700.50	2852.25	1426.1

8. CONCLUSIONS

The spectral analysis of seismic attributes shows an improved understanding of changes in reservoir lithofacies as the geological features within the reservoir interval keep changing from one domain to another.

The combination approach of Gamma, Resistivity and Porosity logs has assisted in identifying the reservoir interval within the two wells (well 4 and 5) at the depth interval of 11,164 to 11,196 ft and 11,048 to 11,097 ft for wells 4 and 5 respectively. Well 4 has a distinct thin sand interval at the depth of 11,193 ft within the reservoir interval where as Well 5 is at depth 11,066.5 ft with a characteristic of low Gamma ray values and high resistivity value.

The results of the coherence spectral analysis of the reservoir interval of the well which is

correspond to 2.752 sec (top of the reservoir) and 2.768 sec (bottom of the reservoir) on seismic section show a major fault at the Nyquist frequency of 50 Hz.

The results from these maps also reveal that processing a coherence attribute in frequency domain rather than relying on horizon picks give better results, then the outcomes of the structural and stratigraphic elements are more evident and well seen.

The study has also revealed that a better geological maps were obtained using coherence in frequency domain (filtered) as the time data is noisy. Hence, a good prospect for hydrocarbon reservoir has been indicated on spectral frequency maps. The study also reveals that the reservoir is a channel fill.

9. RECOMMENDED

It is recommended that for further studies other edge detection attributes such as Semblance, Short response Hilbert transform method (SHLT) should be carried out. This would enable a better resolution or delineation of subsurface stratigraphic features, thus enhancing the hydrocarbon potential and exploration of the study area of the Niger Delta.

ACKNOWLEDGEMENTS

The authors of this research thank Chevron Corporation, Nigeria for making the seismic and well data available for use and research. We are indebted to Exxon Mobil Nigeria for the use of the Petrel Software at its work station at Department of Earth Science, Federal University of Petroleum Resources Effurun, Nigeria and also for the use of her computing facilities.

COMPETING INTERESTS

Authors have declared that no competing interests exist.

REFERENCES

1. Avbovbo AA. Tertiary lithostratigraphy of Niger Delta. American Association of Petroleum Geologists. 1978;10(14):96-200.
2. Etu-Efeotor JO. Fundamentals of petroleum geology, paragrphics. An Imprint of Jeson Services Publisher, Port Harcourt, Nigeria. 1997;146.
3. Fisher R, Gadallah M. Applied exploration geophysicist. Cambridge University Press, London. 2009;310.
4. Gonzalez N, Woods M. Patterns of incidence of oil reserves in the Niger Delta Basin. AAPG Bulletin. 1992;6(5):1251-1259.
5. Hill SJ, Marfurt K, Chopra S. Searching for similarity in a slab of seismic data. The Leading Edge. 1994;33(6):67-77.
6. Offuyah W, Alao O, Olaseni V, Adeoti L. Seismic spectral attributes using coherence and semblance algorithms. Computer Engineering and Intelligent System. 2014;5(9):11-17.
7. Peyton L, Bottjer R, Partyka G. Intepretation of incised valleys using new 3-D seismic techniques: A case history using spectral decomposition and coherency. The Leading Edge. 1998;17:1294-1298.
8. Partyka GA, Gridley JM, Lopez J. Interpretational applications of spectral decomposition in reservoir characterization. The Leading Edge. 1999;18(3):353-360.
9. Short KC, Stauble AJ. Outline of the geology of Niger Delta. American Association of Petroleum Geologists Bulletin. 1986;51(2):761-779.
10. Telford WM, Geldart LP, Sheriff RE. Applied geophysicis. Cambridge University Press, London. 1990;726.
11. Yilmaz O. Seismic data analysis: Processing, inversion, and interpretation of seismic data. Society of Exploration Geophysicists. 2001;2027:5.

© 2018 Olaseni et al.; This is an Open Access article distributed under the terms of the Creative Commons Attribution License (<http://creativecommons.org/licenses/by/4.0>), which permits unrestricted use, distribution, and reproduction in any medium, provided the original work is properly cited.

Peer-review history:

The peer review history for this paper can be accessed here:
<http://www.sciencedomain.org/review-history/23928>